Differential Pressure Sticking of Drill String

J. D. Sherwood
Schlumberger Cambridge Research, Cambridge CB3 0EL, U.K.

The frictional forces acting on a drill string in a borehole can be large if the drill string is embedded in a pastelike filter cake formed at the borehole wall by the drilling fluid. In extreme conditions, the drill string can become stuck, leading to expensive delays in the drilling process. The hydraulic pressure within the wellbore is usually higher than the pore pressure within the rock. This excess pressure is responsible both for the growth of the filter cake, and for the normal force that can hold the drill string against the borehole wall. We obtain estimates of the normal and frictional forces acting on the drill string, based on an analysis of the pressure and concentration profile within the filter cake. The forces can be minimized by ensuring that the cake is highly compressible, so that the bulk of the pressure drop between the borehole and porous rock occurs across a thin boundary layer at the base of the cake. The forces acting on a sphere (rather than a cylindrical drill string) are also modeled, and are compared against experiment. The predicted frictional force is smaller than observed experimentally, but the predicted $t^{3/4}$ growth of the force with time t agrees with experiment.

Introduction

During the drilling of an oil well, the drill string slides deeper into the well as drilling proceeds, and rotates in order to turn the drill bit. In practice the drill string contacts the rock surrounding the hole, especially if the well deviates from the vertical. Drill-string motion is therefore opposed by friction, which, if too large, traps the drill string and causes expensive delays to the drilling process (Bradley et al., 1991).

The borehole contains drilling fluid (Gray and Darley, 1980), which produces a large hydrostatic pressure downhole. This avoids hole collapse due to earth stresses, and prevents the ingress of gas or other pore fluids to the hole. The drilling-fluid density is adjusted so that the downhole hydrostatic pressure is slightly higher than the pressure within the pores of the surrounding rock. This differential pressure drives liquid from the wellbore into the rock. Bentonite and other drilling-fluid particles, which are too large to enter the rock pores, create a low permeability filter cake at the rock surface.

In general, therefore, the drill string interacts not with a rock surface, but with a thin (typically 1–2 mm) filter cake. Whereas in an air bearing the air drives the axle away from the walls, in a well the filtration flow tends to hold the drill string against the rock, thereby increasing the frictional forces. If these forces become sufficiently large, the drill string can be trapped. This is known within the petroleum industry as differential pressure sticking. The differential pressure forces are much larger than typical gravitational forces, so that the orientation of the well (between vertical and horizontal) affects the force mainly by changing the area of contact between filter cake and drill string.

Differential pressure sticking is not the only mechanism whereby drill string can become stuck (Bailey et al., 1991). Other causes include shale swelling, which reduces the diameter of the wellbore (Sherwood and Bailey, 1994), and the snagging of drill collars on irregularities in the borehole. Here, however, we are concerned solely with sticking caused by differential pressure.

Previous work includes large-scale experiments by Quigley et al. (1990) and by Bushnell-Watson and Panesar (1991). Smaller-scale experiments were performed by Annis and Monaghan (1962), Courteille and Zurdo (1985), and Maidla and Wojtanowicz (1990). A theoretical analysis by Outmans (1958) assumed that the mechanical properties of the cake were uniform. However, cakes formed from drilling fluids are highly compressible, and are usually far from uniform. The modeling described here is based on the theory of compressible cakes (Philip and Smiles, 1982) and makes use of measurements of the filter-cake properties reported by Alderman et al. (1991), Sherwood et al. (1991a,b), and by Meeten and Sherwood (1994).

It is generally found that differential pressure sticking is unlikely if the drill string is kept in motion (Bailey et al.,

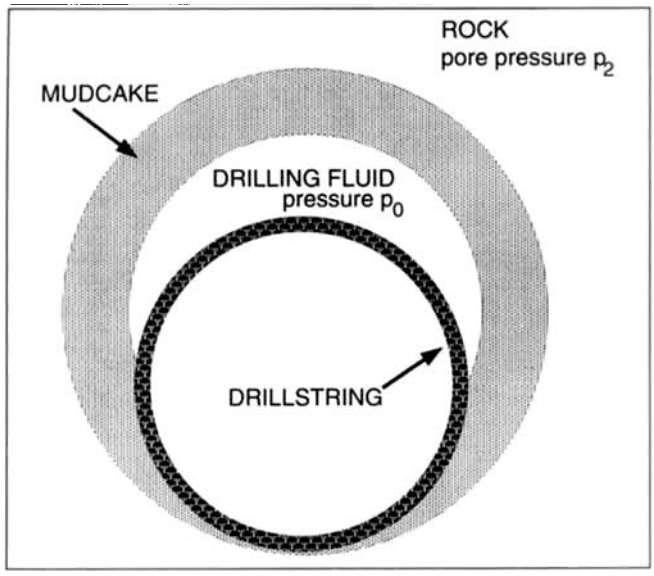

Figure 1. Drill string embedded in the filter cake that covers the rock surface.

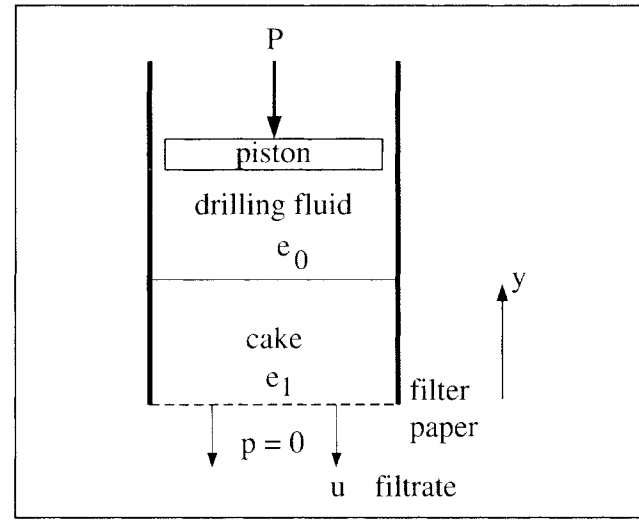

Figure 2. Definition sketch of filtration cell.

1991). A moving drill string tends to erode any filter cake with which it comes into contact. We therefore assume that the drill string is in contact with bare rock, and is brought to rest at time $t = 0$. The filter cake then starts to grow at the rock surface, and around the drill string (see Figure 1). This is the worst possible case. Although the drill string can sink into a preexisting filter cake, this process is slow because of the very low permeability of filter cake.

We first review standard theories for the growth of filter cake in the absence of drill string, assuming (1) that the solids forming the cake, and the liquid filtrate, are incompressible (although the cake itself can be compacted); (2) that the motion of filtrate relative to the solid particles is governed by Darcy's law; (3) that the void ratio e within the cake is a single-valued function of the applied stress; and (4) that the hydraulic permeability of the cake is a function solely of the void ratio e. We then assume that deviatoric stresses are sufficiently small to be neglected during growth of a cake around a cylindrical drill string (or a sphere), and that the void-ratio profile within the cake is negligibly affected by the presence of the cylinder. If the cake is sufficiently thin, the surface of the cylinder may be approximated by a parabola. Previously reported values of the mechanical properties of filter cakes then enable us to estimate the frictional forces acting on a cylinder (or a sphere) embedded in a filter cake. Finally, we describe benchtop experiments that investigate the rate of growth of the frictional forces acting on a sphere around which a filter cake builds up.

Filter-Cake Growth

The rock is usually sufficiently permeable that its hydraulic resistance may be neglected compared with that of the filter cake itself (see the Appendix). Moreover, wellbore curvature can be neglected, since the filter-cake thickness is much smaller than a typical well-bore radius $R_w \simeq 100$ mm. The filtration properties of drilling fluids can therefore be investigated in the laboratory by creating a cake on the surface of a plane filter paper of negligible hydraulic resistance (Figure 2). This process is described by a Lagrangian theory for filter-cake growth, as set out, for example, by Philip and Smiles (1982). We assume that the drilling fluid occupies the region $y > 0$ above the filter paper at $y = 0$. At time $t = 0$ the pressure P (measured relative to atmospheric pressure) is applied to the upper surface of the fluid, and filtrate flows through the filter paper.

The total stress S within the suspension may be represented as a sum

$$S = -pI - \psi I + \Sigma,$$

where p is the fluid pressure within the fluid, ψI is an additional isotropic component due to stress within the matrix of particles, and Σ includes all deviatoric stresses. All velocities are sufficiently slow that inertial effects can be neglected, and applied stresses are sufficiently high that gravity can be neglected. We assume that the applied pressure P is held constant: the y component of the stress balance implies $p + \psi - \Sigma_{yy} = P = \text{constant}$. The matrix of solid particles within a clay filter cake is unable to withstand large shear stresses; more precisely, the shear yield stress is small compared to the isotropic stress ψ (Sherwood et al., 1991b; Meeten, 1994). This also occurs in other aggregated systems of particles (e.g., Channell and Zukoski, 1997). We shall therefore neglect the deviatoric stress Σ_{yy} compared to ψ, so that the y component of the stress balance becomes

$$p + \psi = P = \text{constant}. \tag{1}$$

Although the analysis of one-dimensional filtration presented below holds if we replace ψ throughout by $\psi - \Sigma_{yy}$, we shall later require that the cake flows unhindered into the narrow gap between a cylinder and the rock surface, and we will therefore require that the shear yield stress be small.

We assume that the void ratio e, related to the solids volume fraction ϕ by

$$e = \frac{(1-\phi)}{\phi} = \frac{\text{volume of fluid}}{\text{volume of solid}}, \tag{2}$$

is a single-valued function of ψ. This is a reasonable assumption when the applied pressure is constant (or increases with time), since the void ratio decreases monotonically with time. It would not be true if P were to be reduced during the filtration process, since clay filter cakes, like soils, exhibit hysteresis (e.g., Mitchell, 1976). In the drilling fluid far from the cake, the void ratio e_0 is usually sufficiently large that $\psi_0 = \psi(e_0)$ is negligible, and the pore pressure $p_0 = P - \psi_0 \simeq P$.

Although the filter cake is highly deformable, we assume that the fluid and the solid particles are incompressible. If u_l is the mean velocity of liquid in the y-direction, and u_s that of the solid, the equations of continuity for incompressible particles and fluid become

$$\frac{\partial \phi}{\partial t} = -\frac{\partial}{\partial y}(\phi u_s), \qquad \frac{\partial}{\partial t}(1-\phi) = -\frac{\partial}{\partial y}[(1-\phi)u_l], \tag{3}$$

where we note that $\partial/\partial t$ is a derivative keeping the Eulerian space variable y fixed. We now assume that motion of fluid relative to the particles is governed by Darcy's law (Bear and Bachmat, 1991), and hence

$$q_{\text{rel}} = (1-\phi)(u_l - u_s) = -\frac{k(e)}{\mu}\frac{\partial p}{\partial y}, \tag{4}$$

where q_{rel} is the Darcy velocity of filtrate relative to the (deforming) particle matrix, μ is the viscosity of the filtrate, and the permeability k of the cake is assumed to be a function of the void ratio e.

The equation of continuity is most easily expressed in terms of a Lagrangian coordinate

$$m(y) = \int_0^y \phi \, dy = \int_0^y \frac{dy}{1+e}. \tag{5}$$

Using Eqs. 2-4 we obtain

$$\left.\frac{\partial e}{\partial t}\right|_m = -\frac{1}{\phi^2}\left[\left.\frac{\partial \phi}{\partial t}\right|_y + u_s \frac{\partial \phi}{\partial y}\right] = -\frac{1}{\phi}\frac{\partial q_{\text{rel}}}{\partial y} = -\frac{\partial q_{\text{rel}}}{\partial m},$$

which can alternatively be derived directly by considering fluid fluxes in a Lagrangian frame. Hence, using Darcy's law and Eq. 1

$$\left.\frac{\partial e}{\partial t}\right|_m = -\frac{\partial q_{\text{rel}}}{\partial m} = -\frac{\partial}{\partial m}\frac{k(e)}{\mu}\frac{\partial \psi}{\partial y} = \frac{\partial}{\partial m}\left\{\frac{-k(e)}{\mu(1+e)}\frac{d\psi}{de}\frac{\partial e}{\partial m}\right\}. \tag{6}$$

This is a diffusion equation, and

$$D(e) = -\frac{k(e)}{(1+e)\mu}\frac{d\psi}{de} \tag{7}$$

plays the role of a diffusivity. In the limit $e \to 0$ (or $P \to \infty$) we expect $k(e) \to 0$, and since it becomes increasingly hard to compact the cake any further, $d\psi/de \to \infty$: one or the other of these limits will dominate and determine the behavior of $D(e)$. We shall see later that the behavior of $D(e)$ at high pressure has an important influence upon the pore pressure profile within the filter cake, and hence upon the frictional forces acting on the drill string.

When a constant pressure P is applied at time $t = 0$, there are similarity solutions of Eq. 6 of the form

$$e = e(s) \qquad \text{with} \quad s = mt^{-1/2}, \tag{8}$$

which satisfy

$$\frac{d}{ds}D(e)\frac{de}{ds} + \frac{s}{2}\frac{de}{ds} = 0. \tag{9}$$

The pressure drop across the filter paper is negligible, and hence the fluid at the base of the cake is at atmospheric pressure, $p_1 = 0$. The void ratio e_1 at the filter $y = 0$ therefore satisfies

$$\psi(e_1) = P, \tag{10}$$

and the outer boundary condition for Eq. 9 is $e \to e_0$ as $s \to \infty$.

By solving the similarity equation (Eq. 9), we can predict the profile of void ratio $e(s)$ within the cake. We may then use Eq. 5 to express the profile in terms of a Eulerian similarity variable $r = yt^{-1/2}$.

Although the concentration profile varies continuously as $s \to \infty$, far from the filter paper the void ratio approaches a constant value e_0, with

$$\frac{de}{ds} \sim \exp[-s^2/4D(e_0)] \qquad \text{as} \quad s \to \infty \tag{11}$$

and

$$e_0 - e \sim s^{-1}\exp[-s^2/4D(e_0)] \qquad \text{as} \quad s \to \infty. \tag{12}$$

Integrals of the form $\int_0^\infty f(s)(e_0 - e)\, ds$ therefore converge rapidly as $s \to \infty$. For example, the amount of filtrate lost from the drilling fluid is

$$Q = t^{1/2}S, \tag{13}$$

where

$$S = \int_0^\infty (e_0 - e)\, ds. \tag{14}$$

In practice there will be a value of $s = s_{\max}$ at which the cake may be considered to have an outer boundary. This corre-

sponds in Eulerian space to $r = r_{max} = y_{max} t^{-1/2}$. If D_0 is a typical diffusivity, a typical cake thickness scales as $s_{max} \sim D_0^{1/2}$, $y_{max} \sim D_0^{1/2} t^{1/2}$.

Cake Growth Around a Cylindrical Drill String

Cake growth

Figure 1 shows a filter cake growing around a cylindrical drill string of radius R in contact with the wellbore wall of radius R_w. The filter-cake thickness of a few mm is much smaller than a typical wellbore radius $R_w \simeq 100$ mm. Curvature of the filter cake is therefore unimportant, and far from the drill string the cake will have the void ratio profile of an undisturbed plane cake, with thickness $y_{max} = r_{max} t^{1/2}$. The cake is also thin compared with the radius R of the drill string, and our interest is centered on the region close to the line of contact, in which the distance of separation between the drill string and rock may be approximated by a parabola

$$y = \frac{x^2}{2R}\left(1 - \frac{R}{R_w}\right). \tag{15}$$

The drill string intersects the outer surface of the cake at

$$x_{max} = \left(\frac{2Ry_{max}}{1 - R/R_w}\right)^{1/2}$$

and the region of contact between cake and cylinder subtends a total angle $2\theta_{max}$. The simplified geometry is depicted in Figure 3.

The growth (and consequent deformation) of the filter cake in the narrow gap near the line of contact will be more complex than the simple uniaxial compaction considered earlier. However, shear yield stresses in bentonite drilling fluids and filter cakes are typically an order of magnitude smaller than the stresses required to compact the bentonite gel (Meeten, 1994). Thus one ought to be able to neglect the resulting deviatoric stresses within the bulk of the cake. The wall stresses are harder to dismiss, since the gap between the cylinder and the rock becomes very narrow near the line of contact. Such wall stresses will reduce the ability of the bentonite to flow into this gap. However, the stresses in bentonite drilling fluids (Alderman et al., 1988) and filter cakes (Sherwood et al., 1991b) relax over time scales typically of order 100 s. This allows clay to creep into the gap during cake growth, which occurs over periods of minutes or hours.

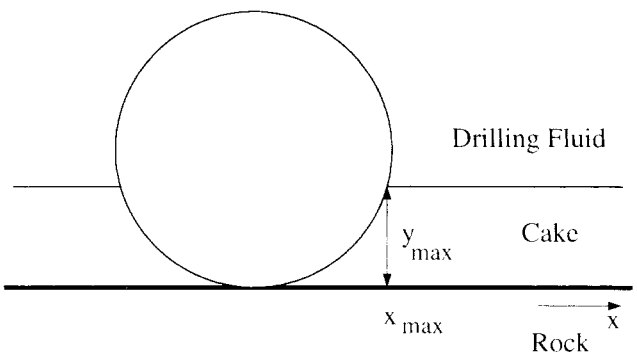

Figure 3. Simplified geometry of a drill string against a plane surface.

In the absence of a full 2-D analysis of cake growth in the complex geometry of Figure 3, we assume that the profiles of particle concentration and pore pressure within the filter cake are unaffected by the presence of the drill string.

Forces acting on a cylinder embedded within the cake

We are neglecting the effect of any deviatoric stresses during the growth of the cake. The stress within the cake around the drill string can therefore be represented by a sum of a pore pressure p and an isotropic matrix stress ψ. By Eq. 1, the integral of $(p + \psi)\boldsymbol{n}$ over the surface $\boldsymbol{n}$ of the cylinder is zero. Thus the cylinder experiences a force from the matrix of clay particles that balances the force due to pressure within the liquid: there is no need for any load to be borne by the rock at the line of contact. This is an important consequence of the assumptions we have made. The frictional force opposing rotation of the cylinder acts between the cylinder and the filter cake, rather than at the line of contact between the cylinder and the rock. Bentonite filter cakes, like soils, do not respond reversibly when stresses are released after compaction (Mitchell, 1976; Lubetkin et al., 1984). Any attempt to lift the cylinder away from the filter cake will tend to separate the clay matrix from the cylinder. The force exerted on the lower surface of the cylinder by the filter cake will then be due to the pore pressure p (rather than $p + \psi$). The uncompacted drilling fluid exerts a total stress P over that part of the cylinder that is not embedded within the cake. The magnitude of the net force per unit length, F_c, holding the drill string against the filter cake is therefore

$$F_c = 2\int_0^{x_{max}} [P - p(y)]\, dx, \tag{16}$$

where $p(y)$ is evaluated at the surface $y(x)$ of the cylinder. With errors $O(\psi_0 x_{max})$ we may modify Eq. 16 to obtain

$$F_c = 2\int_0^{x_{max}} [p_0 - p(y)]\, dx, \tag{17}$$

so that the integrand decays rapidly to zero, and the exact choice of the upper limit x_{max} is not important when evaluating Eq. 17 numerically. Approximating the surface of the drill string by the parabola (Eq. 15), we obtain

$$F_c = t^{1/4}\left(\frac{2R}{1 - R/R_w}\right)^{1/2} I_1, \tag{18}$$

where

$$I_1 = \int_0^{r_{max}} [\psi(r) - \psi_0] r^{-1/2}\, dr. \tag{19}$$

If we take the pressure differential P as a typical order of magnitude for ψ, then we find that the force per unit length $F_c \sim P(tD_0)^{1/4}$. If the cylinder is to rotate about its axis, then friction between the filter cake and the cylinder must be

overcome. The cake itself will yield if friction exceeds the local value of the filter cake yield stress $\tau_y(e)$, and we take $\tau_y(e)$ as an estimate (actually an upper bound) for the frictional force. The excess torque required to rotate the cylinder [above that required to rotate the cylinder in the drilling fluid with yield stress $\tau_y^0 = \tau_y(e_0)$] is therefore

$$T_c = 2R^2 \int_0^{\theta_{\max}} \left[\tau_y(e) - \tau_y^0\right] d\theta, \tag{20}$$

where $\tau_y(e)$ is evaluated at the surface $y(x)$ of the cylinder. In practice, slip may occur at the interface between the filter cake and the cylinder, leading to somewhat lower torques. To evaluate Eq. 20 we require the void-ratio profile $e(y)$ and the yield stress $\tau_y(e)$ as a function of void ratio. However, both shear and compaction of a filter cake require yielding of the matrix of solid particles forming the cake, and experimental measurements of yield stress have typically shown that $\tau_y(e) \simeq \lambda\psi(e)$, where $\lambda \simeq 0.1$ (Sherwood et al., 1991b). Since the cake is thin, we may use the parabolic approximation to obtain the simpler relation

$$T_c = \lambda R F_c. \tag{21}$$

The force required to slide the cylinder along its axis is simply $\lambda F_c = T_c/R$.

Forces acting on a sphere embedded within the cake

Later we describe experiments performed on spheres (rather than cylinders) embedded within filter cakes. We again assume that the void-ratio profile within the cake is unaffected by the presence of the sphere. The normal force holding the sphere against the filter paper is

$$F_s = 2\pi \int_0^{x_{\max}} [P - p(y)]\, x\, dx. \tag{22}$$

Approximating the surface of the sphere by a paraboloid, and again neglecting errors $O(\psi_0 x_{\max}^2)$, Eq. 22 becomes

$$F_s = \frac{2\pi R t^{1/2}}{1 - R/R_w} I_2, \tag{23}$$

where

$$I_2 = \int_0^{r_{\max}} [\psi(r) - \psi_0]\, dr. \tag{24}$$

The sphere cannot slide without creating large plastic deformations of the cake, which we are unable to estimate with any certainty. Rotation of the sphere is, however, possible. If the sphere rotates about an axis normal to the plane of the filter cake, the torque will be

$$\begin{aligned} T_{sn} &= 2\pi \int_0^{x_{\max}} \left[\tau_y(e) - \tau_y^0\right] x^2\, dx, \\ &= \alpha t^{3/4} \end{aligned} \tag{25}$$

where

$$\alpha = \lambda\pi \left(\frac{2R}{1 - R/R_w}\right)^{3/2} I_3 \tag{26}$$

and

$$I_3 = \int_0^{r_{\max}} [\psi(r) - \psi_0]\, r^{1/2}\, dr. \tag{27}$$

The coefficient α is known as the stickance (Reid et al., 1996); a few experimental values are presented below. Rotation about an axis parallel to the surface of the filter cake, assuming that the cake is thin compared to R, leads to a torque

$$\begin{aligned} T_{sp} &= 2\pi R \int_0^{x_{\max}} \left[\tau_y(e) - \tau_y^0\right] x\, dx \\ &= \frac{2\pi R^2 t^{1/2}}{1 - R/R_w} \int_0^{r_{\max}} \left[\tau_y(e) - \tau_y^0\right] dr \\ &\simeq \lambda R F_s. \end{aligned} \tag{28}$$

Estimates Based upon Filter Cake Properties

We require measured values of the mechanical properties of filter cakes in order to evaluate the Eqs. 16–28 for the forces acting on cylinders and spheres embedded within the filter cake.

Here we restrict our attention to drilling fluids based on aqueous suspensions of bentonite. These fluids also contain larger suspended particles, such as barite (a weighting agent) and rock cuttings. Variations in the volume fraction of such suspended solids cause large variations in the properties of the filter cake (Meeten and Sherwood, 1994): a thorough investigation of the effect of solids volume fraction over a wide range of cake compactions has yet to be performed. We first consider unweighted bentonite slurries, and then discuss the differences between these and slurries containing added solids. In order to demonstrate clearly the role of the diffusivity $D(e)$, we shall take this to be the only constitutive relation that is affected by the presence of added solids. At high applied stresses the added solids form a percolating network of incompressible particles, and the diffusivity $D(e)$ becomes large as $e \to 0$. In the absence of added solids, the decrease in permeability $k(e)$ as $e \to 0$ can be sufficient to ensure that $D(e)$ decreases as $e \to 0$.

Unweighted bentonite slurries

We first consider filter cakes of bentonite alone, without any drilled solids or weighting agents. One should be wary of extrapolating any experimental results beyond the range in which they were measured. The void ratio e can be determined as a function of stress ψ by experiment. Fluid is squeezed from a finite sample of drilling fluid (Figure 2) until the cake reaches a final uniform state at the applied filtration pressure P. The amount of fluid remaining within the cake can then be determined by weighing the cake, first when wet, and then after drying at 105°C. Sherwood et al. (1991a) obtained the correlation $e = (P/P_1)^{-0.52}$, with $P_1 = 3.2$ MPa,

whereas Meeten and Sherwood (1994), working at higher pressure on a different bentonite, reported

$$e = e_\infty + (P/P_2)^\gamma, \tag{29}$$

with $e_\infty = 0.707$, $P_2 = 1.868$ MPa, and $\gamma = -0.48$ for an unweighted slurry. Note that Eq. 29 implies that it is impossible to compact the slurry to a void ratio $e < e_\infty$. We shall assume that this residual void ratio is due to water that is bound to the surface of the clay, and that the permeability of the cake becomes small as $e \to e_\infty$. For our purposes this bound water may be regarded as part of the solid within the cake, so we set $e_\infty = 0$ and take

$$e = (P/P_3)^{-0.48}, \tag{30}$$

with $P_3 = 1.7$ MPa in the computations reported here.

The yield stress of concentrated bentonite slurries was measured by Alderman et al. (1991), using a vane. They found

$$\tau_0/\text{MPa} \sim 3\phi^3 \qquad \phi < 0.1. \tag{31}$$

Higher concentrations, up to $\phi = 0.6$, were studied using a squeeze-film technique (Sherwood et al., 1991b). Although the measured yield stresses were somewhat lower than predicted by Eq. 31, it was concluded that Eq. 31 was nevertheless a useful approximation. However, this relation is unlikely to be useful for weighted or solids-laden drilling fluids. It is therefore appropriate to look for a less accurate but more general correlation, based on the ratio λ between the shear yield stress $\tau_0(e)$ and compressive yield stress $\psi(e)$ of a colloidal suspension. This is often reported to be independent of concentration (e.g., Buscall and White, 1987). Meeten (1994) obtained the value $\lambda = 0.09$; Sherwood et al. (1991b) found $\lambda = 0.12$.

The diffusivity $D(e)$ is more difficult to measure. At large values of e it may be determined from measured void-ratio profiles within the cake (Smiles and Harvey, 1973; Smiles and Kirby, 1987; Sherwood et al., 1991a). However, we are particularly interested in the base of the cake, where the void ratio e is small. It is easier to obtain an estimate of $D(e)$ at these small void ratios by means of the outflow inversion method (Smiles and Harvey, 1973; White and Perroux, 1987). Meeten and Sherwood (1994) give results for both weighted and unweighted bentonite slurries. The diffusivity D_1 of the unweighted slurry can be approximated by the hyperbola

$$[\log_{10}(D_1/\text{m}^2\cdot\text{s}^{-1}] + 10.36)^2 = 0.115 + 3.68\,[\log_{10}(e) - 0.32]^2, \tag{32}$$

shown in Figure 4. Note the maximum in D_1, which occurs at $e = 2.09$. Such a maximum has been observed by Smiles and Kirby (1987), and is consistent with the possibility that $D(e) \to 0$ as $e \to 0$. However, the maximum is not always observed (e.g., Kirby and Smiles, 1988; Sherwood, 1997); it is not known whether this is an artifact caused by the difficulty of measuring $D(e)$, or whether the limiting behavior of $D(e)$ merely varies from one slurry to another. The expression (Eq. 29) for $e(P)$ is inconsistent with Eq. 32, which predicts that $D_1 \to 0$ as $e \to 0$, rather than as $e \to e_\infty$. Our decision to take $e_\infty = 0$ has avoided this inconsistency. We could alternatively have adopted Eq. 29, with $e_\infty > 0$, with appropriate adjustment to Eq. 32. This alternative procedure would certainly have been appropriate for a filter cake formed from monodisperse hard spheres, for which we expect $e_\infty > 0.35$ (ordered close packing).

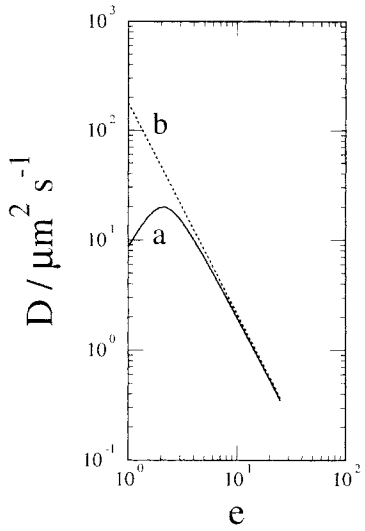

Figure 4. Diffusivities used in the computations.
(a)—— D_1 (32); (b) ····· D_2 (33).

We also need to know the void-ratio profile within the cake. This can be measured either by a cake-slicing technique (Meeten, 1993; Sherwood et al., 1991a), or by tomography (Horsfield et al., 1989). However, it is more convenient here to use $D_1(e)$, as given by Eq. 32, in the similarity equation (Eq. 9) in order to predict the void-ratio profile at any given filtration pressure P.

Effect of added solids

In general, a drilling fluid will contain not only bentonite but also larger solid particles, such as barite or rock cuttings. Much less is known about the mechanical properties of filter cakes made from such a fluid, though it is generally expected that the yield stress of such cakes will be higher, leading to larger frictional torques.

Meeten and Sherwood (1994) studied a bentonite slurry to which 5% (by volume) barite had been added, so that the initial solids-volume fraction in the drilling fluid was $\phi_s = 0.07$. The void ratio $e(P)$ could be represented by Eq. 29 with $e_\infty = 0.36$, $P_2 = 0.21$ MPa, and $\gamma = -0.44$. Added solids also modify both the magnitude and concentration dependence of the diffusivity $D(e)$. Meeten and Sherwood (1994) showed that the diffusivity of a solids-laden cake is higher than that of an unweighted cake. This leads to thicker filter cakes, and consequently to larger frictional forces, as discussed earlier.

The dependence of D on the void ratio e is modified because the matrix of large solid particles within the cake eventually becomes load-bearing at sufficiently high compaction. The compressibility of the cake is then reduced. The unstressed bentonite gel within the pores of the matrix of large solid particles has a higher permeability then the compacted

bentonite in an unweighted cake. These changes to the cake compressibility and permeability reduce any tendency for the diffusivity to decrease when the pressure differential increases to very high values. This difference between the behavior of weighted and unweighted filter cakes was observed by Meeten and Sherwood (1994). In order to isolate this one feature, we shall consider a filter cake in which the void ratio is given, as before, by Eq. 30, but the diffusivity D_2 takes the form

$$\log_{10}(D_2/\mathrm{m}^2\cdot\mathrm{s}^{-1}) = -9.75 - 1.92\log_{10}(e). \qquad (33)$$

This is shown in Figure 4, and we see that it is similar to D_1 (Eq. 32) when $e > 0.6$, but has no maximum. We shall again rely on computations to provide us with the void-ratio profile within the cake.

Predictions of the Model

We shall assume that the void ratio of the drilling fluid is $e_0 = 40$. From Eqs. 9, 30 and 32 we can compute void-ratio profiles e within the cake as a function of the Lagrangian similarity variable s. The computations were started away from the cake, using Eqs. 11 and 12 for the initial conditions. The profiles are shown in Figure 5. We can convert the Lagrangian similarity variable s to a Eulerian variable r by Eq. 5, and hence obtain profiles $e(r)$ in Eulerian space, as shown in Figure 6. As the filtration pressure $P \to \infty$, the void ratio e and diffusivity $D(e)$ both tend to 0 at the base of the cake, where, by Eq. 9, de/ds becomes large. A thin, low-permeability boundary layer develops at the base of the cake, across which most of the drop in pore pressure occurs. Similar behavior is predicted in a model of the filter cake formed from emulsions (Sherwood, 1993), and this explains the low permeability of filter cakes formed from drilling fluids made of water-in-oil emulsions. Note also that an increase in pressure does not necessarily lead to a thicker cake in real (Eulerian) space. We see from Figure 6 that at high pressure the base of the cake is highly compacted, and the cake appears to be thinner than the low-concentration cakes formed at lower pressure.

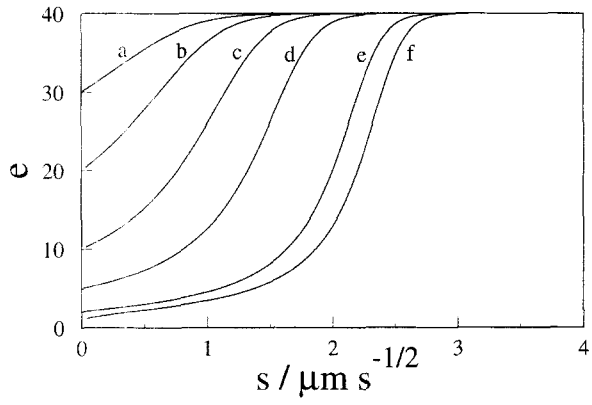

Figure 5. Profiles of void ratio e within the cake as a function of the Lagrangian similarity variable $s = mt^{-1/2}$.

Diffusivity D_1 (32), with $e(P)$ given by (30). Void ratio at base of cake and corresponding filtration pressure: (a) $e_1 = 30$, $P = 1.4$ kPa; (b) $e_1 = 20$, $P = 3.4$ kPa; (c) $e_1 = 10$, $P = 14$ kPa; (d) $e_1 = 5$, $P = 60$ kPa; (e) $e_1 = 2$, $P = 0.4$ MPa; (f) $e_1 = 1$, $P = 1.7$ MPa.

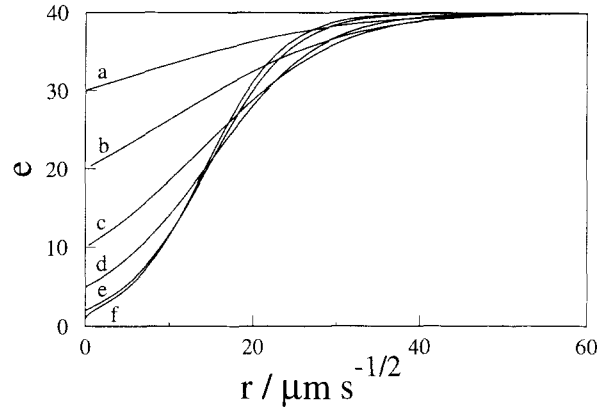

Figure 6. Profiles of void ratio e within the cake as a function of the Eulerian similarity variable $r = yt^{-1/2}$.

Diffusivity D_1 (32), with $e(P)$ given by (30). Void ratio at base of cake and corresponding filtration pressures as in Figure 5.

If we change to the diffusivity D_2 given by Eq. 33, we obtain the results in Figure 7, rather than those in Figure 5. High filtration pressures do not create a layer of low permeability: the filtration rate is increased, and the cake is thicker than before. Moreover, the pressure drop across the cake will no longer be concentrated at the thin boundary layer.

Figure 8a shows the desorptivity S, computed by Eq. 14, as a function of the applied pressure. Note that results for the two diffusivities D_1 and D_2 are similar at pressures $P < 0.3$ MPa, corresponding to a void ratio $e_1 = 2.3$, close to the value at which D_1 is maximum. If the pressure is increased further, the desorptivity corresponding to D_1 increases only slowly, because of the low-permeability boundary layer at the base of the cake.

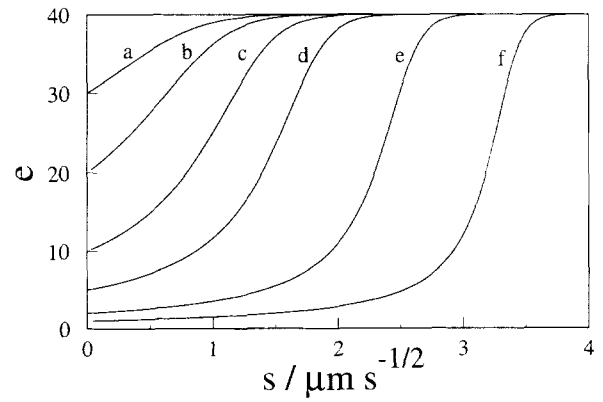

Figure 7. Profiles of void ratio e within the cake as a function of the Lagrangian similarity variable $s = mt^{-1/2}$.

Diffusivity D_2 (33), with $e(P)$ given by (30). Void ratio at base of cake and corresponding filtration pressures as in Figure 5.

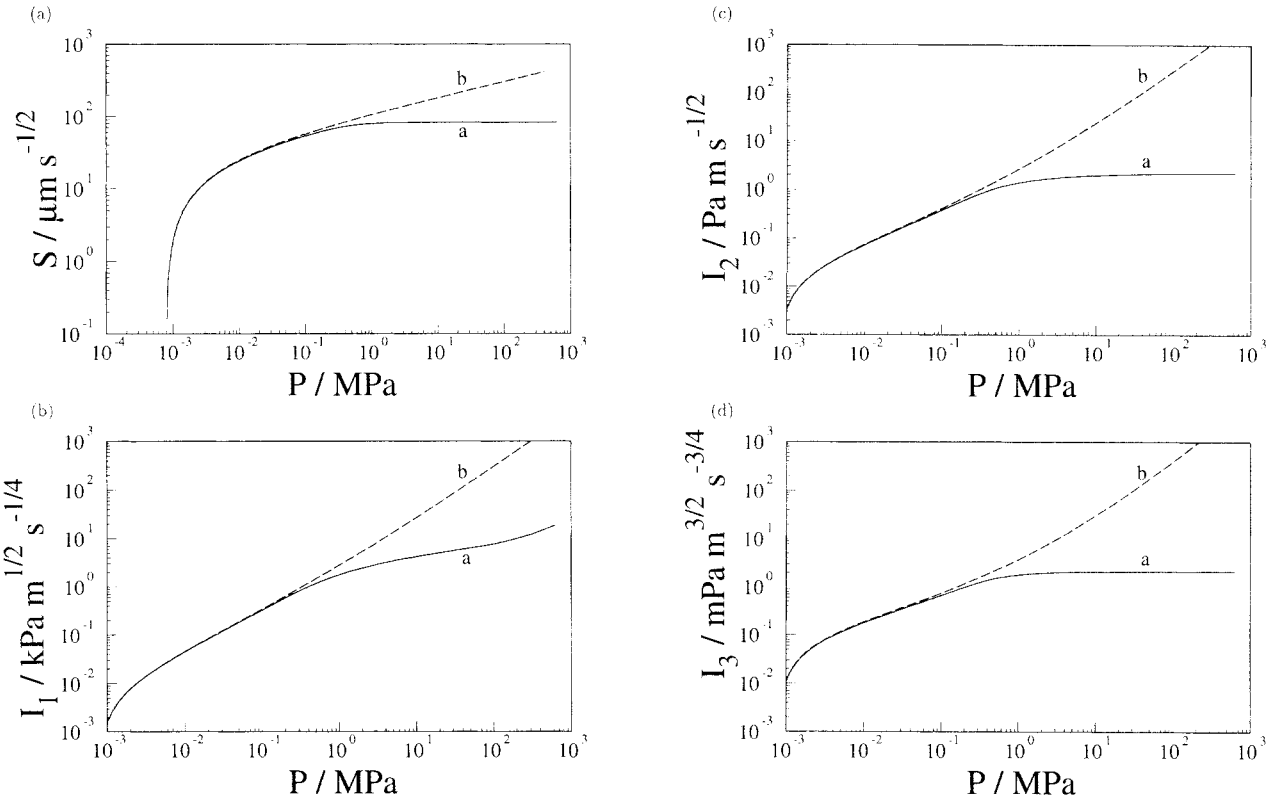

Figure 8. Desorptivity S, defined by (14), and the integrals (b) I_1 (19), (c) I_2 (24), and (d) I_3 (27), as functions of the filtration pressure P.

The drilling fluid has initial void ratio $e_0 = 40$, with void ratio $e(P)$ given by (30) and diffusivity (a) —— D_1 (32), (b) - - - D_2 (33).

Figure 8b shows the integral I_1, defined by Eq. 19, evaluated as a function of P. Again, the two diffusivities predict similar results at pressure $P < 0.3$ MPa. At high pressures the diffusivity D_1 leads to a thin boundary layer, outside of which little change occurs as the pressure is increased. However, the factor $r^{-1/2}$ in the integrand (Eq. 19) makes I_1 sensitive to changes within the boundary layer. Similar results for I_2 and I_3 are shown in Figure 8c and 8d. We see that I_2 and I_3 become independent of pressure at high pressure, when computed using diffusivity D_1.

In an incompressible filter cake, we expect the cake height to grow as $P^{1/2}$, and the pressure will vary linearly across the cake. We therefore expect $I_1 \propto P^{5/4}$, $I_2 \propto P^{3/2}$, and $I_3 \propto P^{7/4}$. The diffusivity D_2 corresponds to a cake that becomes increasingly hard to compress as the void ratio is reduced: we might therefore expect the behavior of such a cake to approach that of an incompressible cake. However, the outer part of the cake is always compressible, and it is this part of the cake that dominates the integral I_3. We see from Figure 8 that the integrals I_1, I_2, and I_3 evaluated for diffusivity D_2 increase more rapidly than P as $P \to \infty$, but less rapidly than expected for an incompressible cake.

Experiments

Experiments in which a filter cake was allowed to grow around a sphere of radius 19.05 mm have been reported by Reid et al. (1996). The drilling fluids contained barite and drilled solids, and had an initial solids volume fraction ϕ_s. The torque T_{sn} required to turn the sphere was measured as a function of the time t over which the cake had formed. Results, taken at filtration pressures $P = 1.4$ MPa, 4.2 MPa, and 5.6 MPa in a drilling fluid with solids volume fraction $\phi_s = 0.1$ are shown in Figure 9. We see that T_{sn} is approximately linear in $t^{3/4}$, as predicted by Eq. 25, and that the stickance α increases with filtration pressure P. The de-

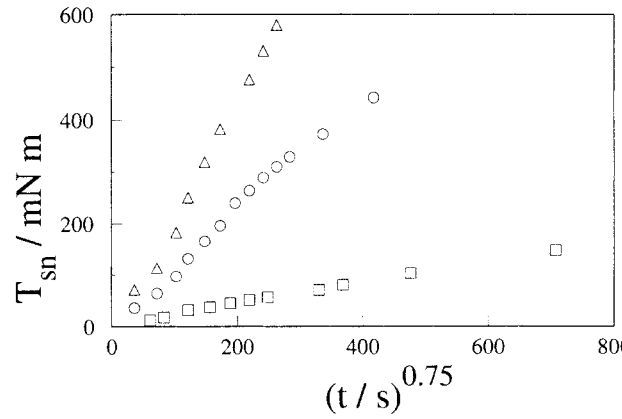

Figure 9. Torque T_{sn} required to turn a sphere of radius $R = 19.05$ mm about an axis normal to the filter paper, as a function of time t.

Solids volume fraction $\phi_s = 0.1$, filtration pressure (a) $P =$ 200 psi □; (b) 600 psi ○; (c) 800 psi △.

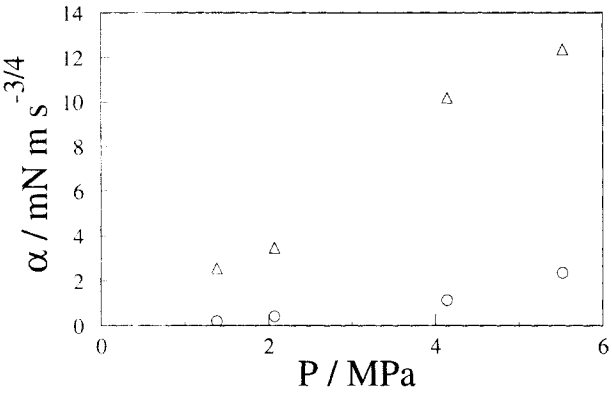

Figure 10. Stickance α as a function of filtration pressure P.

Solids volume fraction (a) $\phi_s = 0.1$ ○; (b) $\phi_s = 0.2$ △.

pendence of α on P is shown in Figure 10 for two drilling fluids, with $\phi_s = 0.1$ and $\phi_s = 0.2$. As expected from the previous general discussion, α increases with both P and with ϕ_s.

In the experiments R_w is infinite (corresponding to a plane surface) and $R = 19.05$ mm. At 1.4 MPa, $I_3 = 4.9$ mPa m$^{3/2}$ s$^{-3/4}$ when computed using D_2, and hence, by Eq. 26, $\alpha = 0.1\lambda$ mN m s$^{-3/4}$, which may be compared with the experimental value $\alpha = 0.2$ mN m s$^{-3/4}$ obtained from Figure 9. Experiment and theory only agree if $\lambda = 2$, a value that we reject as excessively large. Part of the discrepancy is due to the high solids volume fraction $\phi_s = 0.1$ in the drilling fluid used to produce the results of Figure 9, so that the diffusivity D_2 used in the computations is unrealistically small. We see from Figure 10 that the stickance increases rapidly with solids-volume fraction, and drilling fluids with high solids-volume fraction were therefore of most interest to Reid et al. (1996). The assumption that the concentration profile within the cake is undisturbed by the presence of the sphere is also a possible cause of the discrepancy. This assumption becomes dubious when the drilling fluid contains large solid particles, which are unable to flow into the narrow gap between the sphere and filter.

Conclusions

The results presented here tell a consistent story. If the filter cake is highly compressible (i.e., if the diffusivity of the filter cake decreases as the void ratio becomes small), at high filtration pressures a thin boundary layer develops at the base of the cake, within which the solids concentration is high and the permeability is low. If the rock pore pressure decreases, not only will the rate of cake growth hardly increase, but the pore pressure in the outer portion of the cake will be unchanged. Consequently the forces acting on drill string embedded within the cake increase only slightly, and the integrals I_1 (Eq. 19), I_2 (Eq. 24), and I_3 (Eq. 27) increase only slowly with the filtration pressure P. Thus a drilling fluid should create a thin, highly compressible filter cake if differential pressure sticking is to be avoided. If, on the other hand, the cake contains a high proportion of rock cuttings or other large solid particles, the matrix of particles tends to become rigid at high compaction. If the rock pore pressure decreases, not only will the cake grow more rapidly, but the pore pressure will vary throughout the cake. Both these features tend to increase the forces leading to sticking.

Acknowledgments

I thank my colleagues G. Meeten, P. Way, and S. Davies for the experimental data presented in Figures 9 and 10.

Literature Cited

Alderman, N. J., D. Ram Babu, T. L. Hughes, and G. Maitland, "The Rheological Properties of Water-Based Drilling Fluids," *Proc. Int. Congr. Rheology*, Vol. 1, Sydney, p. 140 (1988).

Alderman, N. J., G. H. Meeten, and J. D. Sherwood, "Vane Rheometry of Bentonite Gels," *J. Non-Newtonian Fluid Mech.*, **39**, 291 (1991).

American Petroleum Institute, "Recommended Practice Standard Procedure for Field Testing Drilling Fluids," API Recommended Practice 13B, 12th ed., API, Washington DC (1988).

Annis, M. R., and P. H. Monaghan, "Differential Pressure Sticking —Laboratory Studies of Friction Between Steel and Mud Filter Cake," *J. Pet. Technol.*, SPE 151, 537 (1962).

Bailey, L., T. Jones, J. Belaskie, J. Orban, M. Sheppard, O. Houwen, S. Jardine, and D. McCann, "Stuck Pipe: Causes, Detection and Prevention," *Oilfied Rev.*, **3**(4), 13 (1991).

Bear, J., and Y. Bachmat, *Introduction to Modeling of Transport Phenomena in Porous Media*," Kluwer, Dordrecht, The Netherlands (1991).

Bradley, W. B., D. Jarman, R. S. Plott, R. D. Wood, T. R. Schofield, R. A. Auflick, and D. Cocking, "A Task Force Approach to Reducing Stuck Pipe Costs," *Proc. SPE/IADC Drilling Conf.*, SPE 21999, Society of Petroleum Engineers, Richardson, TX (1991).

Buscall, R., and L. W. White, "The Consolidation of Concentrated Suspensions. Part 1 The Theory of Sedimentation," *J. Chem. Soc., Faraday Trans. 1*, **83**, 873 (1987).

Bushnell-Watson, Y. M., and S. S. Panesar, "Differential Sticking Laboratory Tests Can Improve Mud Design," *Proc. Annu. Tech. Conf.*, SPE 22549, Society of Petroleum Engineers, Richardson, TX (1991).

Carslaw, H. S., and J. C. Jaeger, *Conduction of Heat in Solids*, 2nd ed., Oxford Univ. Press, Oxford, U.K. (1959).

Channell, G. M., and C. F. Zukoski, "Shear and Compressive Rheology of Aggregated Alumina Suspensions," *AIChE J.*, **43**, 1700 (1997).

Courteille, J. M., and C. Zurdo, "A New Approach to Differential Sticking," *Proc. Annu. Tech. Conf.*, SPE 14244, Society of Petroleum Engineers, Richardson, TX (1985).

Gray, G. R., and H. C. H. Darley, *Composition and Properties of Oil Well Drilling Fluids*, 4th ed., Gulf Pub., Houston (1980).

Horsfield, M. A., E. J. Fordham, C. Hall, and L. D. Hall, "^{1}H NMR Imaging Studies of Filtration in Colloidal Suspensions," *J. Magn. Reson.*, **81**, 593 (1989).

Kirby, J. M., and D. E. Smiles, "Hydraulic Conductivity of Aqueous Bentonite Suspensions," *Aust. J. Soil Sci.*, **26**, 561 (1988).

Lubetkin, S. D., S. R. Middleton, and R. H. Ottewill, "Some Properties of Clay-Water Dispersions," *Philos. Trans. R. Soc. Lond. A*, **311**, 353 (1984).

Maidla, E. E., and A. K. Wojtanowicz, "Laboratory Study of Borehole Friction Factor with a Dynamic-Filtration Apparatus," *SPE Drilling Eng.*, **5**, 247 (1990).

Meeten, G. H., "A Dissection Method for Analysing Filter Cakes," *Chem. Eng. Sci.*, **48**, 2391 (1993).

Meeten, G. H., "Shear and Compressive Yield in the Filtration of a Bentonite Suspension," *Colloids Surf.*, **82**, 77 (1994).

Meeten, G. H., and J. D. Sherwood, "The Hydraulic Permeability of Bentonite Suspensions with Granular Inclusions," *Chem. Eng. Sci.*, **49**, 3249 (1994).

Mitchell, J. K., *Fundamentals of Soil Behaviour*, Wiley, New York (1976).

Outmans, H. D., "Mechanics of Differential Pressure Sticking of Drill Collars," *Trans. Soc. Pet. Eng. AIME*, **213**, 263 (1958).

Philip, J. R., and D. E. Smiles, "Macroscopic Analysis of the Behavior of Colloidal Suspensions," *Adv. Colloid Interface Sci.*, **17**, 83 (1982).

Quigley, M. S., A. K. Dzialowski, and M. Zamora, "A Full Scale Wellbore Friction Simulator," *Proc. SPE/IADC Drilling Conf.*, SPE 19958, Society of Petroleum Engineers, Richardson, TX (1990).
Reid, P. I., G. H. Meeten, P. W. Way, P. Clark, B. D. Chambers, and A. Gilmour, "Mechanisms of Differential Sticking and a Simple Well Site Test for Monitoring and Optimizing Drilling Mud Properties," *Proc. SPE/IADC Drilling Conf.*, SPE 35100, Society of Petroleum Engineers, Richardson, TX (1996).
Sherwood, J. D., "A Model for Static Filtration of Emulsions and Foams," *Chem. Eng. Sci.*, **48**, 3355 (1993).
Sherwood, J. D., "The Initial and Final Stages of Compressible Filtercake Compaction," *AIChE J.*, **43**, 1488 (1997).
Sherwood, J. D., and L. Bailey, "Swelling of Shale Around a Cylindrical Wellbore," *Proc. Roy. Soc. Lond. A*, **444**, 161 (1994).
Sherwood, J. D., G. H. Meeten, C. A. Farrow, and N. J. Alderman, "The Concentration Profile Within Non-Uniform Mudcakes," *J. Chem. Soc. Faraday Trans.*, **87**, 611 (1991a).
Sherwood, J. D., G. H. Meeten, C. A. Farrow, and N. J. Alderman, "Squeeze-Film Rheometry of Non-Uniform Mudcakes," *J. Non-Newtonian Fluid Mech.*, **39**, 311 (1991b).
Smiles, D. E., and E. G. Harvey, "Measurement of Moisture Diffusivity of Wet Swelling Systems," *Soil Sci.*, **116**, 391 (1973).
Smiles, D. E., and J. M. Kirby, "Aspects of One-Dimensional Filtration," *Sep. Sci. Technol.*, **22**, 1405 (1987).
White, I., and K. M. Perroux, "Use of Sorptivity to Determine Field Soil Hydraulic Properties," *Soil Sci. Soc. Amer. J.*, **51**, 1093 (1987).

Appendix: The Hydraulic Resistance of the Rock

In the laboratory, a filter cake is usually formed on a thin filter paper of negligible hydraulic resistance. In a wellbore, the filter cake builds up on porous rock, which, although (usually) more permeable than the filter cake, is also of much greater thickness. We can estimate the relative importance of the rock resistance compared to that of the filter cake by means of a simple study of 1-dimensional compressible flow.

Let P be the pressure in the filtrand, p_1 the fluid pressure at the base of the filter cake, and p_2 the pore pressure far from the well. If p_1 is constant then, as shown by Eq. 13, the flux of filtrate through the growing filter cake is

$$v = \frac{1}{2} S t^{-1/2}$$

where the desorptivity S is a function of the pressure difference $P - p_1$ across the cake. In a laboratory filter cell $p_1 = 0$ (atmospheric pressure).

The filter cake can easily be deformed by rearrangement of solid particles within it, and it is therefore appropriate to neglect compressibility of the filtrate when studying cake growth. However, this is harder to justify in the almost rigid, porous rock. We therefore suppose that the bulk modulus of the pore fluid is K, and that the rock porosity ϕ is a function of the pore pressure p, with

$$\phi = \phi_0[1 + \beta(p - p_2)],$$

where ϕ_0 and p_0 are the porosity and pore pressure far from the wellbore. Fluid flow is assumed to obey Darcy's law, and hence the volume flux v is given by

$$v = -\frac{k_r}{\mu}\frac{\partial p}{\partial y},$$

where k_r is the permeability of the rock and μ the viscosity of the filtrate. The pore pressure obeys a diffusion equation

$$\frac{\partial p}{\partial t} = -\frac{K_e}{\phi_0}\frac{\partial v}{\partial x} = D_r \frac{\partial^2 p}{\partial y^2}, \tag{34}$$

where

$$K_e = \frac{K}{1 + \beta K} \quad \text{and} \quad D_r = \frac{k_r K_e}{\mu \phi_0}. \tag{35}$$

We assume that the pore pressure is initially constant and equal to p_2 everywhere, and that at time $t = 0$ the pressure at $y = 0$ changes to p_1. If p_1 is constant, the diffusion equation (Eq. 34) has solution

$$p = p_1 + (p_2 - p_1)\,\mathrm{erf}\left[\frac{1}{2} y (D_r t)^{-1/2}\right]$$

and the flux into the rock at $y = 0$ is

$$v = A(p_1 - p_2)t^{-1/2},$$

where

$$A = k_r \mu^{-1} (\pi D_r)^{-1/2}.$$

It is clear that we can construct a solution to the full problem of rock and filter cake, with constant pressure p_1 at the rock/cake boundary, and with continuity of fluid velocity, if

$$S = 2A(p_1 - p_2). \tag{36}$$

Now S is a function of the pressure difference $P - p_1$ across the cake. A simple limiting case occurs when the cake is incompactible, with void ratio e_c and permeability k_c. In this case

$$S = 2B^{1/2}(P - p_1)^{1/2},$$

where

$$B = \frac{2k_c(e_0 - e_c)}{\mu(e_c + 1)}.$$

Hence continuity of flux (Eq. 36) at the cake/rock boundary is satisfied if

$$B(P - p_1) = A^2(p_1 - p_2)^2,$$

and $P - p_1 \gg p_1 - p_2$ (i.e., most of the pressure drop occurs across the filter cake) if

$$P - p_1 \gg B/A^2 = \frac{2\pi k_c(e_0 - e_c)K_e}{(e_c + 1)\phi_0 k_r}.$$

However, bentonite filter cakes are compactible, with a desorptivity S that varies only slowly with the pressure differential. If we take S to be constant, Eq. 36 implies that the pressure drop across the rock will be negligible if $P - p_1 \gg S/2A$. We take as typical values $S = 60\ \mu\text{m}\cdot\text{s}^{-1/2}$, $k_r = 10^{-13}\ \text{m}^2 = 100$ mD, $\phi = 0.1$, $\mu = 10^{-3}$ Pa·s. In Eq. 35, β is typically $O(K^{-1})$, so we take $K_e = K = 2$ GPa. This leads to $D_r \simeq 2$ and $S/2A \simeq 0.75$ MPa. This is similar to the differential pressure (100 psi) recommended in the American Petroleum Industry (API) standard laboratory filtration test (American Petroleum Industry, 1988). In practice, flow from a wellbore is radial, rather than linear. A full analysis of radial flow requires a numerical calculation, and reveals that the resistance of the filter cake dominates the flow even more than suggested by the estimates obtained earlier. In the absence of a filter cake, when $t \gg R_w^2/Dr$ the flux into the rock decays as $(\ln t)^{-1}$ (Carslaw and Jaeger, 1959), that is, more slowly than the $t^{-1/2}$ assumed here, and thus we have overestimated the effective resistance of the rock surrounding the wellbore. Taking a typical wellbore radius to be $R_w \simeq 120$ mm, and $D_r \simeq 2$, the changeover from linear to radial diffusion occurs at a time $t \sim R_w^2/D_r \sim 0.007$ s.

Manuscript received Aug. 4, 1997, and revision received Nov. 21, 1997.